Progress In Electromagnetics Research C, Vol. 84, 189–200, 2018

A Wideband Circularly Polarized Antenna with Wide Beamwidth for GNSS Applications

Chao Li*, Fushun Zhang, Fan Zhang, and Kaiwen Yang

Abstract—A wideband circularly polarized antenna with wide half power beamwidth (HPBW) and 3 dB axial-ratio beamwidth (ARBW) is proposed in this paper. The circularly polarized (CP) radiation is realized by feeding two crossed printed dipoles through a wideband feeding network with broadband 90° phase shift. By adding a thick substrate layer and a notched-corner metal cavity around the antenna, the impedance bandwidth (VSWR < 2) is greatly enhanced. The HPBW of the proposed antenna is greater than 110° while the ARBW is greater than 130° in the operating band, simultaneously. The overall dimension of the antenna is only $70 \times 70 \times 36\,\text{mm}^3$. The measured results show that the impedance bandwidth of the proposed antenna reaches 54.7% (1.06 GHz–1.86 GHz) while the AR bandwidth (AR < 3 dB) is 48.6% (1.08 GHz–1.78 GHz). As such, the proposed antenna can be widely used in various global navigation satellite system (GNSS) applications.

1. INTRODUCTION

Nowadays, circularly polarized (CP) antennas have been widely used in various global satellite navigation systems (GNSS) such as the global positioning system (GPS) and compass satellite navigation system (CNSS). In order to improve the coverage area and stabilize the receiving signal in GNSS applications, wide HPBW and ARBW are very valuable for the antenna. In order to increase the HPBW, many techniques have been used such as extending the substrate beyond the ground plane in [1], loading auxiliary radiators in [2], loading with curved microstrip resonant structure in [3], reshaping the ground plane of the antenna in [4] and adopting dual-ring cavity in [5]. However, the antennas mentioned above have relatively large dimension, and the impedance and AR bandwidths are relatively narrow. On the other hand, many studies have been done to achieve wide ARBW such as loading a magneto-electric dipole in [6, 7], introducing parasitic structures around the antenna in [8, 9], adopting asymmetric microstrip antennas with integrated circular or stub patches in [10, 11] and combining two pairs of linear dipoles in a square contour in [12]. Nevertheless, the HPBW of these antennas is narrower than 80°. Above all, it is necessary to get a wideband CP antenna with wide HPBW and ARBW at the same time.

In this paper, by adding a thick substrate layer and a notched-corner cavity around two crossed dipoles fed by a wideband feeding network, a wideband CP antenna with wide HPBW and ARBW is achieved. Details of the proposed antenna design are presented in Section 2.

2. ANTENNA GEOMETRY AND DESIGN PROCESS

2.1. Antenna Geometry

The geometry of the proposed antenna is shown in Figure 1, which is mainly composed of two crossed printed dipoles, a feeding network and a notched-corner metal cavity. The overall dimension of the

Received 12 April 2018, Accepted 28 May 2018, Scheduled 7 June 2018

* Corresponding author: Chao Li (lichao972@126.com).

The authors are with the National Laboratory of Antennas and Microwave Technology, Xidian University, Xi'an, Shaanxi 710071, China.

proposed antenna is only $70 \times 70 \times 36\,\text{mm}^3$ or $0.32 \times 0.32 \times 0.17\lambda^3$, where λ is the corresponding free-space wavelength at 1.4 GHz. The printed dipoles are etched on the bottom layer of the FR4 substrate with a thickness of 1 mm and a relative permittivity of 4.4. Two coaxial cables are used to feed the dipoles. One arm of each dipole is connected to the outer conductor while the other arm is connected to the inner conductor through a small microstrip line bridge above the dipoles. Meanwhile, the other arm of each dipole is shorted to the ground via a metal post. The two crossed connecting bridges are one over the other and are etched on two substrates both with a thickness of 0.5 mm and a relative permittivity of 2.65. A thick FR4 substrate layer with a thickness of 30 mm is added between the dipoles and the feeding network. Figure 1(d) shows the layout of the feeding network which consists of a 3-dB Wilkinson power divider and a broadband 90° phase shifter in [13]. The feeding network is composed of two substrates both with a thickness of 1 mm and a relative permittivity of 2.65. The feeding lines are etched on the middle layer of the substrates while the ground planes are etched on the up and bottom layers. It can be regarded as a stripline feeding network. Finally, a notched-corner metal cavity is introduced around the antenna. Four nonmetallic supporting screws are used to connect the antenna

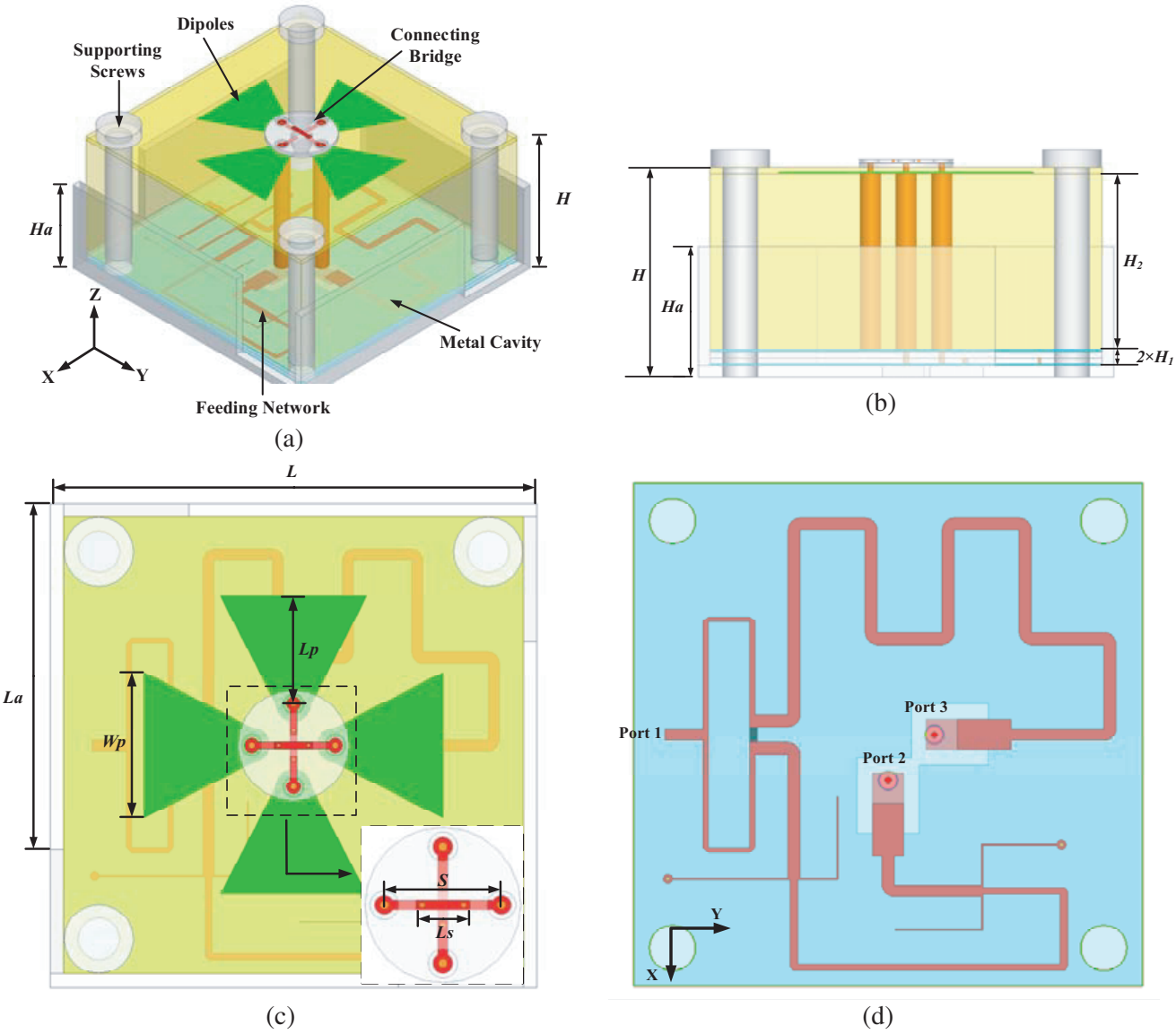

Figure 1. Geometry of the proposed antenna. (a) 3D view. (b) Side view. (c) Top view. (d) Feeding network.

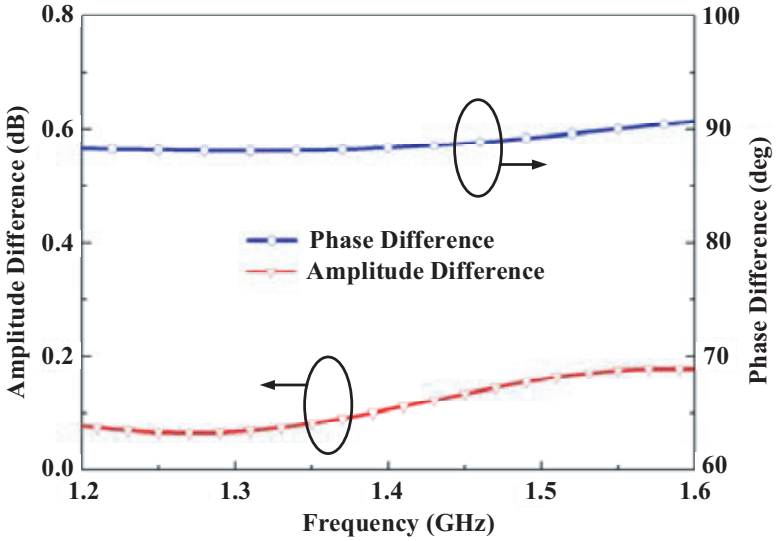

Figure 2. Simulated phase and amplitude differences of the output ports.

and the metal cavity.

The simulated phase and amplitude differences of the proposed feeding network are presented in Figure 2. As shown in Figure 2, a consistent phase difference of approximately $90° \pm 5°$ and an amplitude difference of less than 0.2 dB ($|S_{21}| - |S_{31}| < 0.2$ dB) are achieved in the frequency range of 1.2–1.7 GHz.

The ANSYS high frequency structure simulator (HFSS) is used to investigate and optimize the antenna configuration. The optimized antenna design parameters are as follows: $L = 70$ mm, $La = 50$ mm, $Lp = 15.5$ mm, $Ls = 5.5$ mm, $Wp = 21$ mm, $S = 12$ mm, $H = 36$ mm, $Ha = 22$ mm, $H_1 = 1$ mm, $H_2 = 30$ mm.

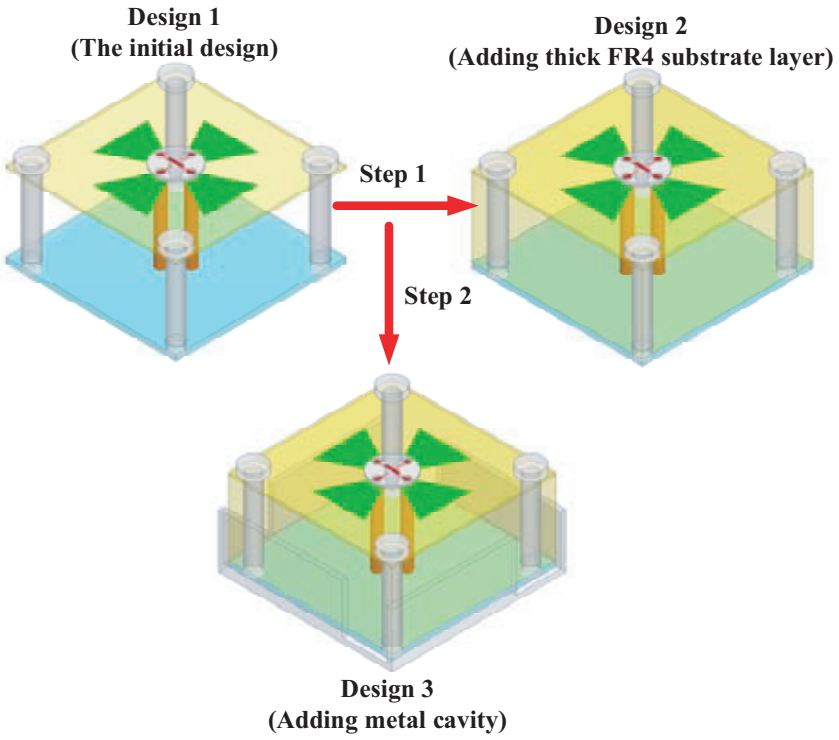

Figure 3. The design process of the proposed antenna.

2.2. Antenna Design Process

The design process of the proposed antenna (without the feeding network) is presented in Figure 3. The initial design (Design 1) is only composed of two crossed dipoles Then a thick FR4 substrate layer with thickness of H_2 is added in Design 2. Finally, a notched-corner metal cavity is introduced in Design 3. All of the three designs use the same substrates with the same dimension of $70 \times 70 \times 36\,\text{mm}^3$.

Figure 4 shows the simulated VSWR at one feeding port of the three antenna designs without the feeding network. It can be seen that from Design 1 to Design 2, the resonant frequency shift downwards. The main reason is that the relative profile of the antenna is increased due to adding the thick FR4 substrate layer. From Design 2 to Design 3, the resonant frequency at high band of the proposed antenna shifts downwards a little while one more resonant frequency at low band is generated due to the introduction of the notched-corner metal cavity so that the impedance bandwidth of the proposed antenna gets greatly enhanced.

Figure 5 shows the simulated surface current distributions on vertical portions of the cavity at 1.16 GHz and 1.58 GHz, which are the resonant frequencies at low and high bands of the proposed antenna respectively. Due to the coupling between the dipoles and the metal cavity, the surface currents

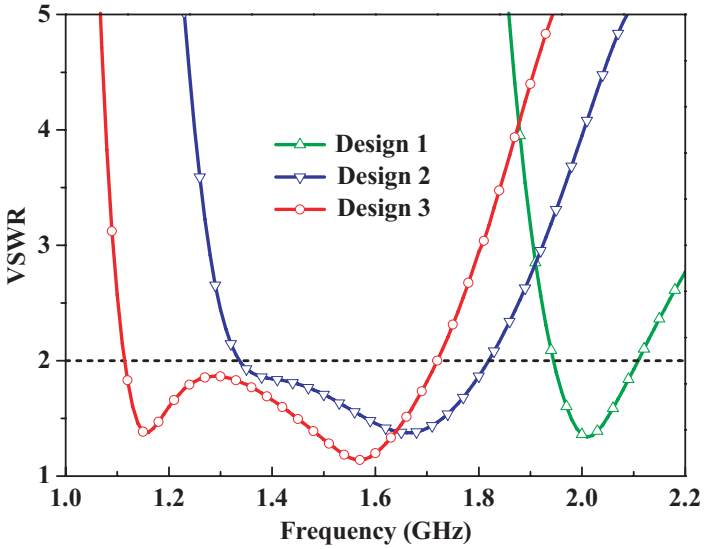

Figure 4. Simulated VSWR of the three antenna designs.

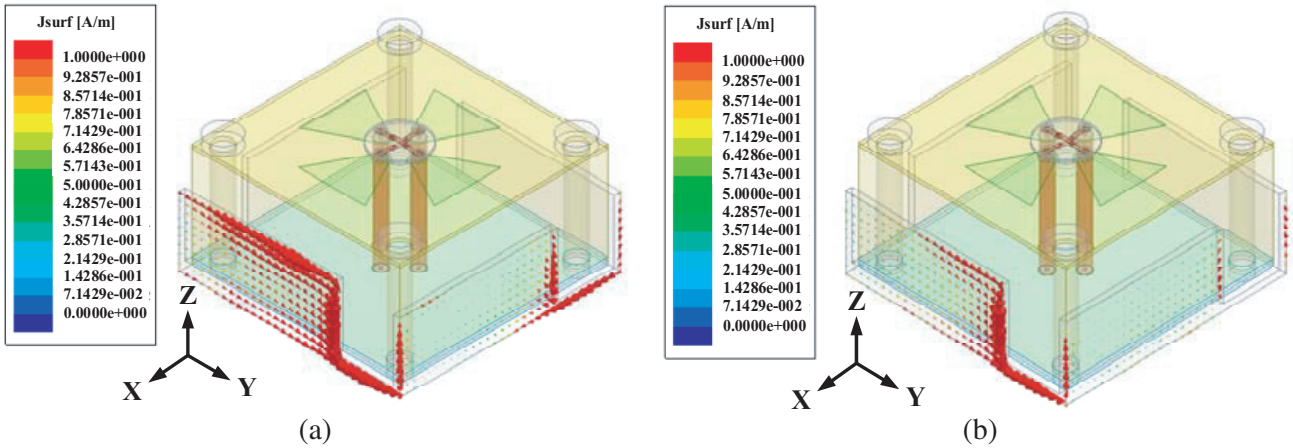

Figure 5. Simulated current distributions of the proposed antenna at (a) 1.16 GHz and (b) 1.58 GHz.

on the vertical portions of the cavity are generated. As can be seen in Figure 5, the currents at 1.16 GHz are stronger than the currents at 1.58 GHz. It means that the electrical length of the dipole is increased due to the coupling currents on the cavity so that the impedance matching gets better at low band. Meanwhile, due to the vertical currents, the radiated electric fields are enhanced at low elevation angles so that wide HPBW and ARBW are generated. The normalized radiation patterns at center frequencies of the three designs (Design 1 at 2 GHz, Design 2 at 1.6 GHz and Design 3 at 1.4 GHz) in the XOZ plane are plotted in Figure 6. From Design 1 to Design 3, the HPBW of the proposed antenna gets enlarged from 78° to 124° as shown in Figure 6.

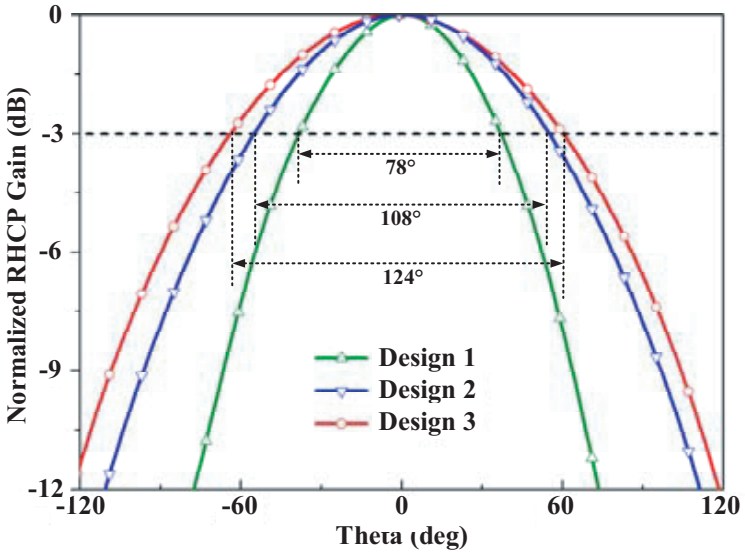

Figure 6. Simulated normalized radiation patterns at center frequencies of the three designs.

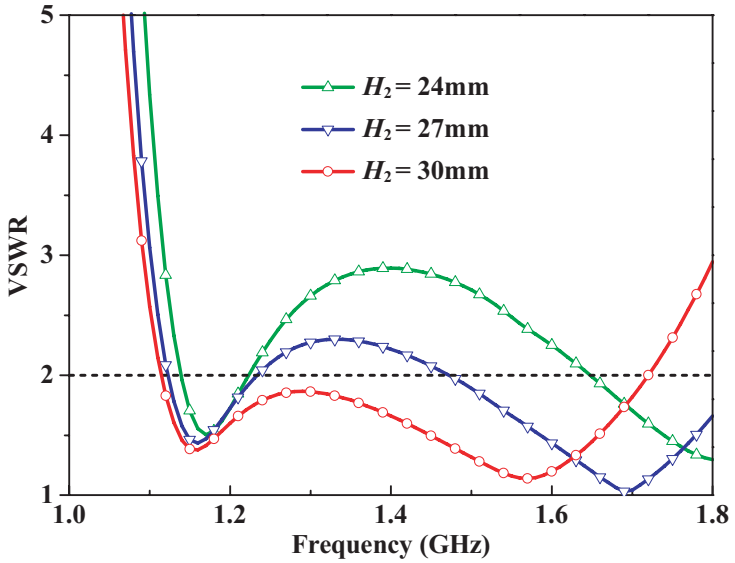

Figure 7. Simulated VSWR for various values of H_2.

3. PARAMETRIC STUDY

According to the design process of the proposed antenna, the introduction of the thick FR4 substrate layer and the notched-corner metal cavity are the main ways to enhance the impedance bandwidth of the proposed antenna, thus the height H_2 of the substrate layer, the height Ha and the length La of the notched portion of the cavity have been studied.

The simulated VSWR at one feeding port of the proposed antenna without the feeding network for various values of H_2 is plotted in Figure 7. With H_2 varying from 24 mm to 30 mm, the resonant frequency at high band shifts downwards a lot while the resonant frequency at low band shifts a little. This phenomenon means that the thick FR4 substrate layer mainly influences the resonant frequency at high band.

Figure 8 and Figure 9 show the simulated VSWR for various values of Ha and La, respectively.

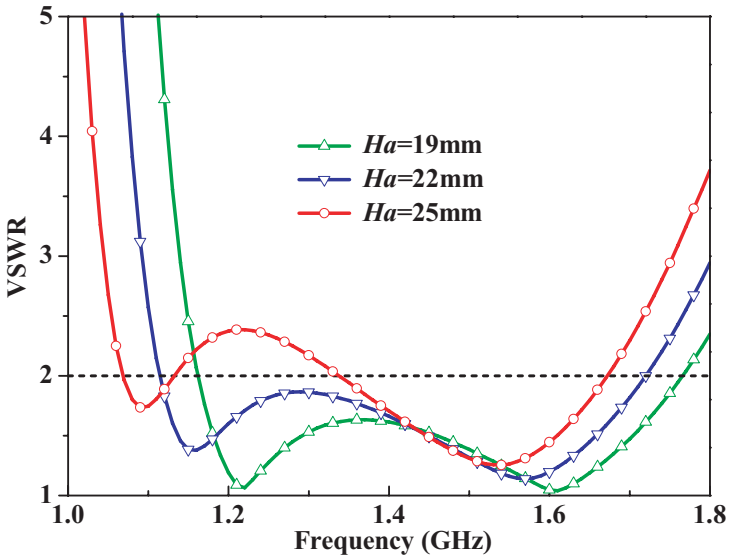

Figure 8. Simulated VSWR for various values of Ha.

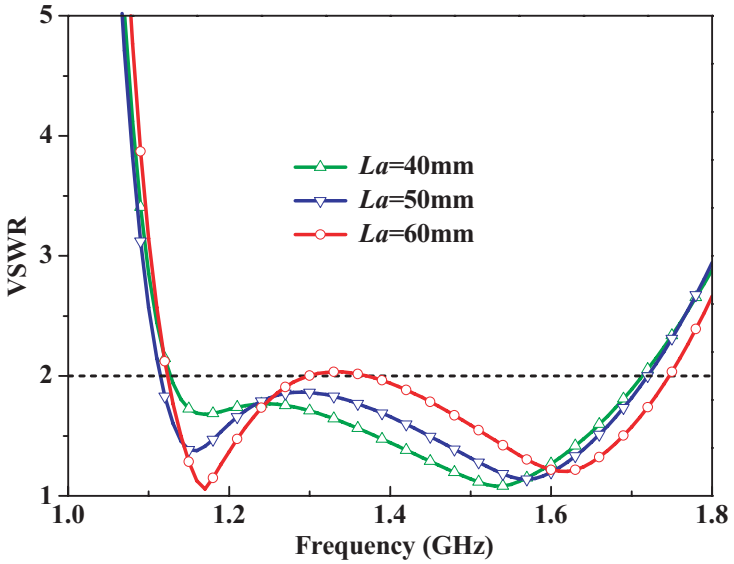

Figure 9. Simulated VSWR for various values of La.

With Ha varying from 19 mm to 25 mm in Figure 8, the resonant frequency at high band shifts a little while the resonant frequency at low band shifts downwards. It means that the height Ha is the main parameter to influence the resonant frequency at low band. In Figure 9, with La varying from 40 mm to 60 mm, the impedance matching at low band gets better. For comprehensive consideration of the impedance bandwidth and the impedance matching at low band, the Ha and La are chosen as 22 mm and 50 mm respectively.

4. SIMULATED AND MEASURED RESULTS

A prototype of the proposed antenna is fabricated and measured as shown in Figure 10. The VSWR of the proposed antenna is measured with the Wiltron 37269A vector network analyzer while the radiation patterns and ARs are measured in an anechoic chamber.

The simulated and measured VSWRs of the proposed antenna are plotted in Figure 11, and a good agreement can be seen between the simulated and measured results. The measured impedance bandwidth (VSWR < 2) of the proposed antenna is ranging from 1.06 GHz to 1.86 GHz with a relative

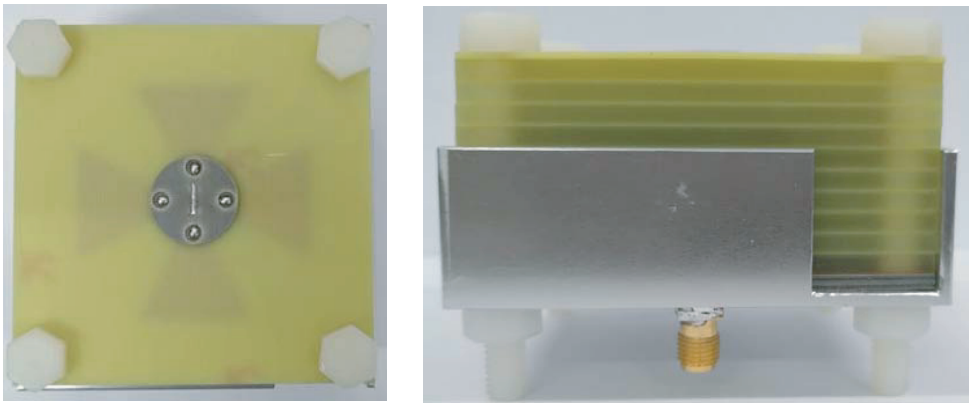

(a) (b)

Figure 10. Prototype of the proposed antenna. (a) Top view. (b) Side view.

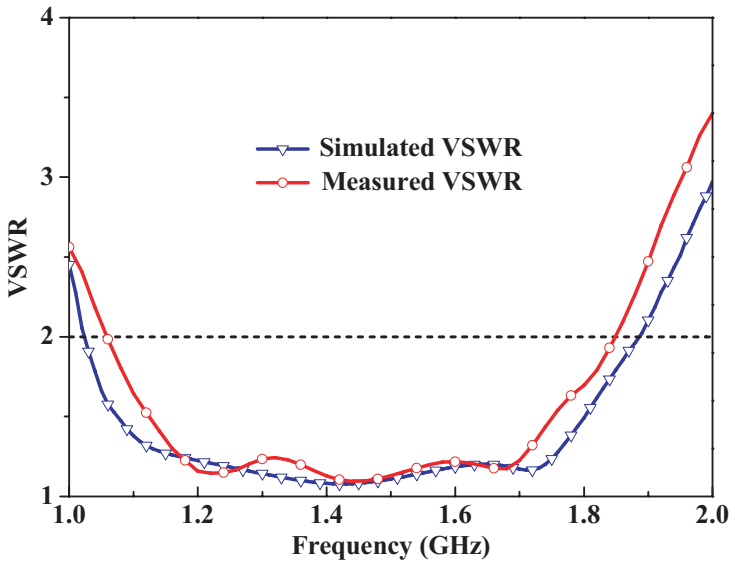

Figure 11. Simulated and measured VSWR of the proposed antenna.

bandwidth of 54.7%.

The simulated and measured ARs at the boresight direction of the proposed antenna are plotted in Figure 12. The measured AR bands (AR < 3 dB) of the proposed antenna is ranging from 1.08 GHz to 1.78 GHz with a relative bandwidth of 48.6%.

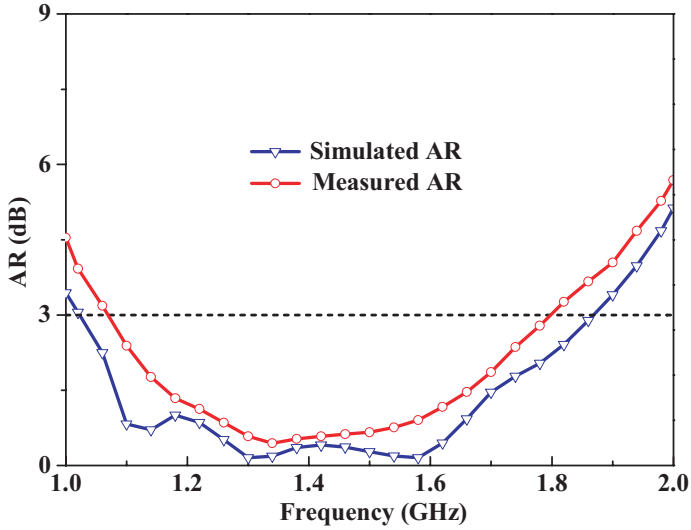

Figure 12. Simulated and measured AR at the boresight direction of the proposed antenna.

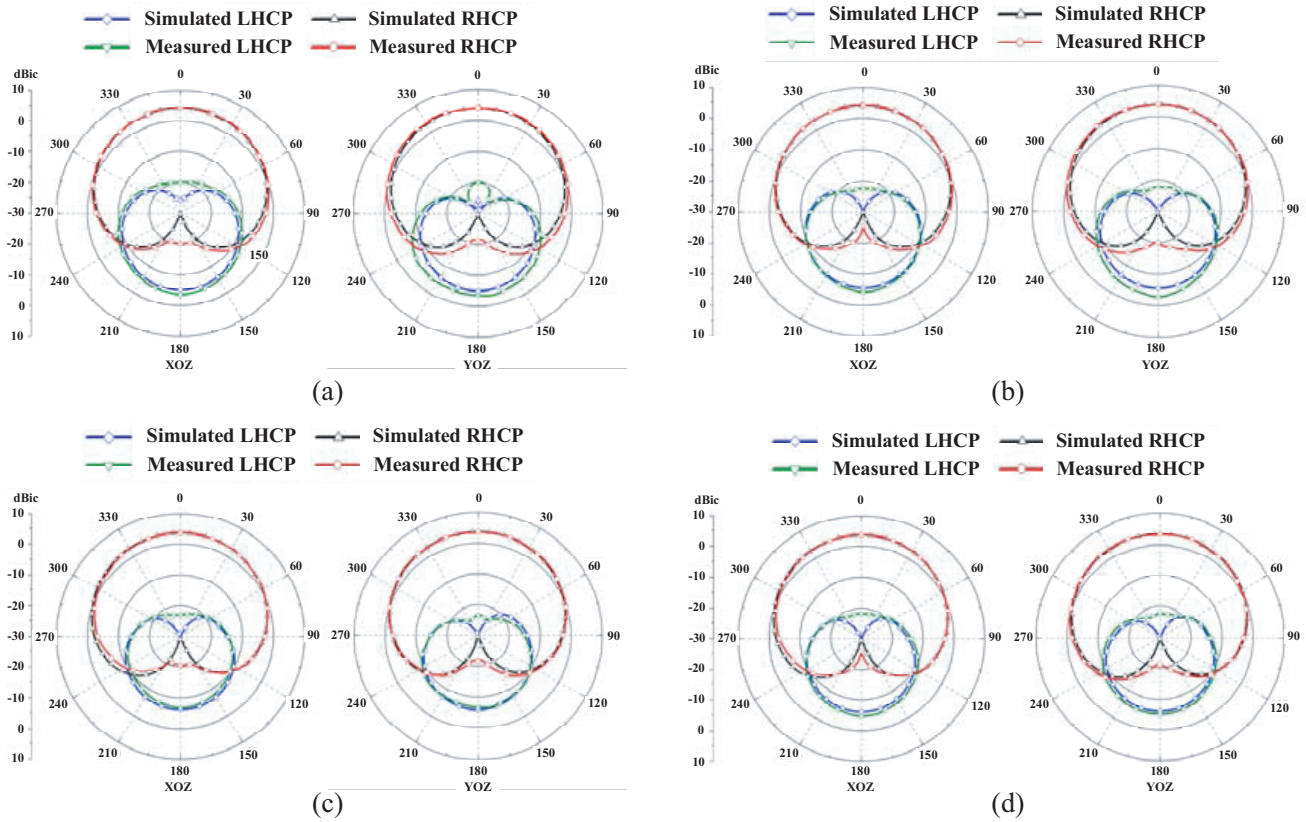

Figure 13. Simulated and measured radiation patterns at (a) 1.227 GHz, (b) 1.268 GHz, (c) 1.561 GHz, (d) 1.575 GHz.

The simulated and measured radiation patterns at 1.227 GHz, 1.268 GHz, 1.561 GHz and 1.575 GHz which are the center frequencies of the GPS-L2, CNSS-B3, CNSS-B1 and GPS-L1 bands respectively in XOZ and YOZ planes are plotted in Figure 13.

The simulated and measured ARs at these frequencies in XOZ and YOZ planes are plotted in Figure 14. The measured radiation performances including RHCP gains, HPBW and ARBW at these frequencies are listed in Table 1.

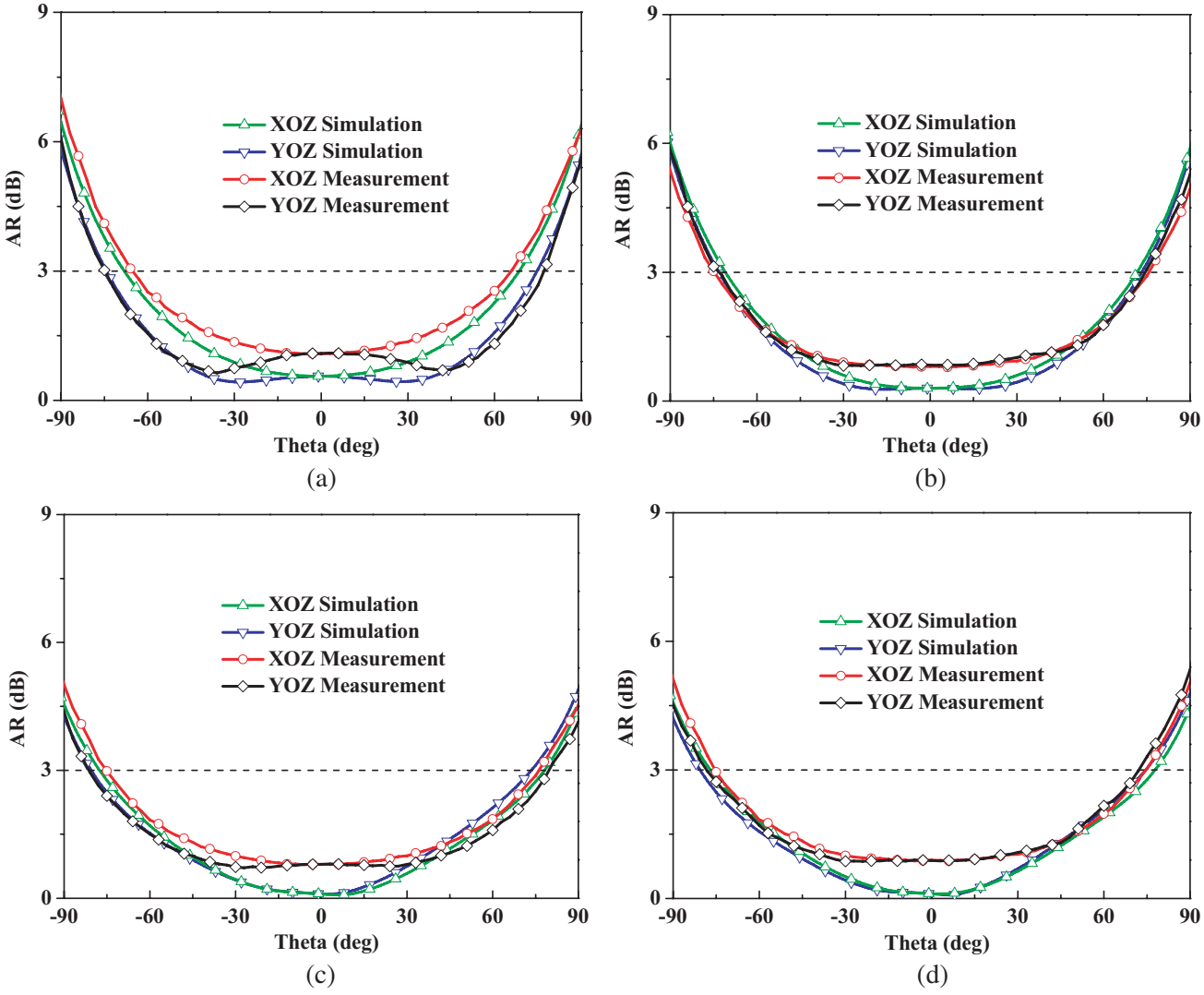

Figure 14. Simulated and measured AR at (a) 1.227 GHz, (b) 1.268 GHz, (c) 1.561 GHz, (d) 1.575 GHz.

Table 1. Measured RHCP gains, HPBW and ARBW of the proposed antenna.

Frequency (GHz)	RHCP Gain (dB)	HPBW (°)		ARBW (°)	
		XOZ	YOZ	XOZ	YOZ
1.227	4.0	116	118	132	152
1.268	3.9	120	116	150	146
1.561	3.5	123	129	151	161
1.575	3.5	124	126	150	150

The simulated and measured RHCP gains and radiation efficiencies at the boresight direction are plotted in Figure 15. As can be seen in Figure 15, the measured RHCP gains of the proposed antenna are greater than 3.5 dB while the radiation efficiencies are larger than 70% in the frequency band ranging from 1.1 GHz to 1.7 GHz.

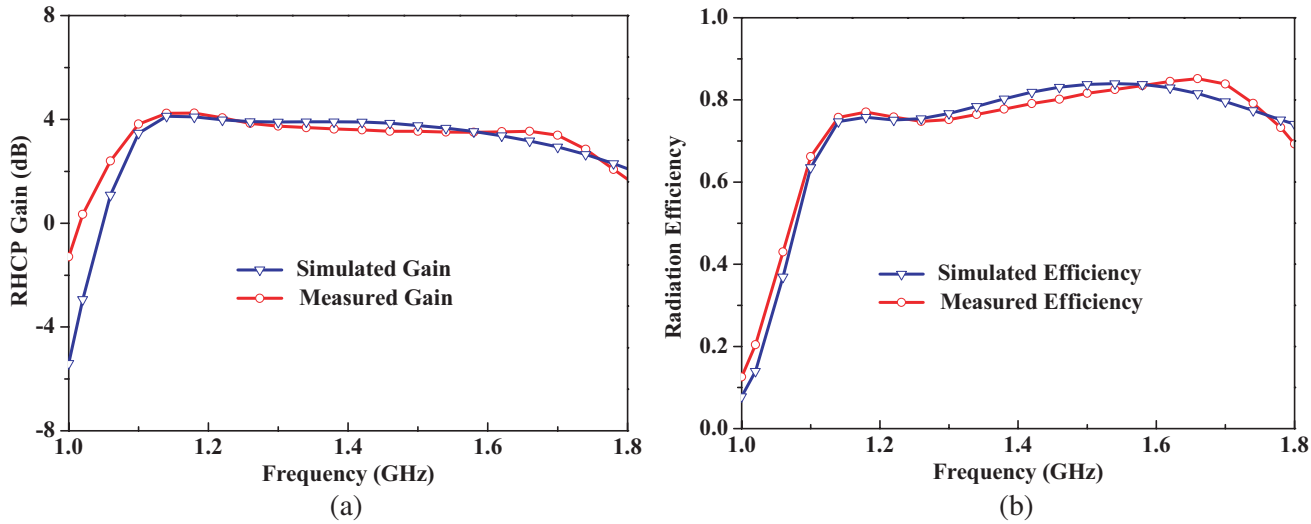

Figure 15. Simulated and measured boresight (a) RHCP gains and (b) radiation efficiencies.

The simulated and measured HPBW and ARBW of the proposed antenna are plotted in Figure 16. As shown in Figure 16, the HPBW is greater than 110° while the ARBW can reach up to larger than 130° in the frequency band ranging from 1.2 GHz to 1.7 GHz. Discrepancies between the measured and simulated results are likely due to substrate and measurement errors.

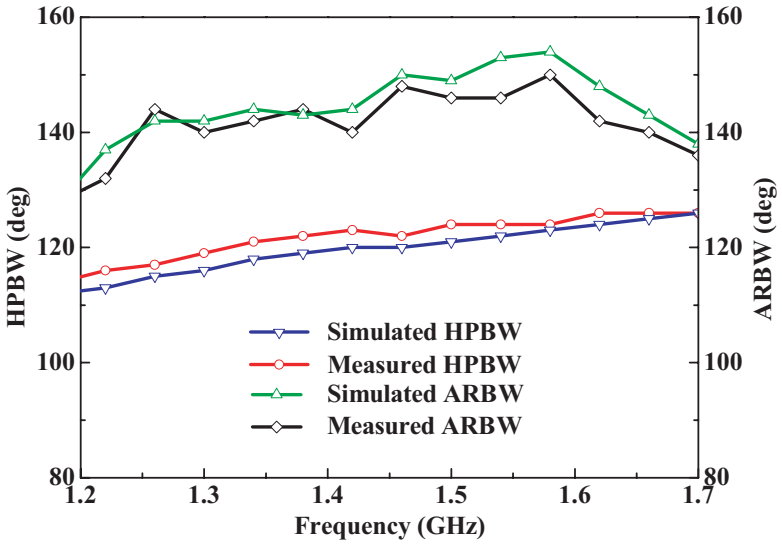

Figure 16. Simulated and measured HPBW and ARBW of the proposed antenna.

Table 2 shows the comparison of the performance between the previous antenna designs and those of the proposed antenna. As can be seen in Table 2, the proposed antenna has a wide impedance bandwidth and a wide AR bandwidth with wide HPBW and ARBW. Meanwhile, the overall dimension of the proposed antenna is relatively compact compared with the other antennas.

Table 2. Performances comparison between the previous antennas and the proposed antenna.

Antenna Structure	Overall Dimension (λ^3)	Impedance Bandwidth (%)	AR Bandwidth (%)	HPBW (°)	ARBW (°)	Gain (dB)
Proposed	$0.32 \times 0.32 \times 0.17$	54.7	48.6	110	130	3.5
Ref. [3]	$0.70 \times 0.70 \times 0.02$	14.2	No mention	150	147	2.5
Ref. [4]	$0.79 \times 0.79 \times 0.12$	1.3	0.8	130	131	-0.6
Ref. [6]	$0.64 \times 0.64 \times 0.16$	59.8	26.8	70	165	8.0
Ref. [7]	$0.97 \times 0.97 \times 0.25$	41	33	85	87	6.3
Ref. [10]	$0.37 \times 0.37 \times 0.02$	3.5	1.5	≤ 100	180	5.2
Ref. [12]	$0.53 \times 0.53 \times 0.004$	32.5	7.5	≤ 100	126	5.0

5. CONCLUSION

A wideband CP antenna with wide beamwidth including HPBW and ARBW is proposed in this paper. By adding a thick substrate layer and a notched-corner metal cavity around the antenna which is composed of two crossed dipoles fed by a wideband feeding network, a wide impedance bandwidth of 54.7% and an AR bandwidth of 48.6% are achieved. Meanwhile, at the operating band, the HPBW is greater than 110°, and the ARBW is larger than 130° with a relatively compact dimension of $0.32 \times 0.32 \times 0.17\lambda^3$. With these performances, the proposed antenna can be a good candidate for various GNSS applications.

REFERENCES

1. Bao, X. L. and M. J. Ammann, "Dual-frequency dual circularly-polarised patch antenna with wide beamwidth," *Electron. Lett.*, Vol. 44, No. 21, 1233–1234, 2008.
2. Chen, Z. N., W. K. Toh, and X. M. Qing, "A microstrip patch antenna with broadened beamwidth," *Microw. Opt. Technol. Lett.*, Vol. 50, No. 7, 1885–1888, 2008.
3. Cao, W. Q., B. N. Zhang, A. J. Liu, T.-B. Yu, D.-S. Guo, Y. Wei, and Z.-P. Qian, "A low-profile CP microstrip antenna with broad beamwidth based on loading with curved microstrip resonant structures," *Journal of Electromagnetic Waves and Applications*, Vol. 26, Nos. 11–12, 1602–1610, 2012.
4. Su, C. W., S. K. Huang, and L. Zhu, "CP microstrip antenna with wide beamwidth for GPS band application," *Electron. Lett.*, Vol. 43, No. 20, 1062–1063, 2007.
5. Zuo, S. L., L. Yang, and Z. Y. Zhang, "Dual-band CP antenna with a dual-ring cavity for enhanced beamwidth," *IEEE Antennas Wireless Propag. Lett.*, Vol. 14, 867–870, 2015.
6. Ta, S. X. and I. Park, "Crossed dipole loaded with magneto-electric dipole for wideband and wide-beam circularly polarized radiation," *IEEE Antennas Wireless Propag. Lett.*, Vol. 14, 358–361, 2015.
7. Mak, K. M. and K. M. Luk, "A circularly polarized antenna with wide axial ratio beamwidth," *IEEE Trans. Antennas Propag.*, Vol. 57, No. 10, 3309–3312, 2009.
8. Duan, X. D. and R. L. Li, "A novel center-fed dual-band circularly polarized antenna for GNSS applications," *Proc. IEEE Antennas Propag. Soc. Int. Symp. (APSURSI)*, 1015–1016, Memphis, TN, USA, 2014.
9. Tan, T. S., Y. L. Xia, and Q. Zhu, "A novel wide beamwidth and circularly polarized microstrip antenna loading annular dielectric superstrate with metal ring," *Proc. IEEE Antennas Propag. Soc. Int. Symp. (APSURSI)*, 1883–1884, Memphis, TN, USA, 2014.

10. Nasimuddin, Y. S. Anjani, and A. Alphones, "A wide-beam circularly polarized asymmetric-microstrip antenna," *IEEE Trans. Antennas Propag.*, Vol. 63, No. 8, 3764–3768, 2015.
11. Vignesh, S. B., Nasimuddin, and A. Alphones, "Stubs-integrated-microstrip antenna design for wide coverage of circularly polarised radiation," *IET Microwaves, Antennas and Propagation*, Vol. 11, No. 4, 444–449, 2017.
12. Luo, Y., Q.-X. Chu, and L. Zhu, "A low-profile wide-beamwidth circularly-polarized antenna via two pairs of parallel dipoles in a square contour," *IEEE Trans. Antennas Propag.*, Vol. 63, No. 3, 931–936, 2015.
13. Eom, S. Y. and H. K. Park, "New switched-network phase shifter with broadband characteristics," *Microw. Opt. Technol. Lett.*, Vol. 38, No. 4, 255–257, 2008.